The impact of oxic degradation on long chain alkyl diol distributions in Arabian Sea surface sediments

Marta Rodrigo-Gámiz [a,b,*], Sebastiaan W. Rampen [a], Stefan Schouten [a,c], Jaap S. Sinninghe Damsté [a,c]

[a] NIOZ Royal Netherlands Institute for Sea Research, Department of Marine Organic Biogeochemistry, and Utrecht University, P.O. Box 59, 1790 AB, Den Burg, Texel, The Netherlands (Sebastiaan.Rampen@nioz.nl; Stefan.Schouten@nioz.nl; Jaap.Damste@nioz.nl)

[b] Present address: Instituto Andaluz de Ciencias de la Tierra (IACT), CSIC-Universidad de Granada, Spain

[c] Utrecht University, Faculty of Geosciences, Department of Earth Sciences, Geochemistry, Utrecht, The Netherlands

* Corresponding author: Marta Rodrigo-Gámiz, Instituto Andaluz de Ciencias de la Tierra (IACT), CSIC-UGR, Avda. de las Palmeras 4, 18100 Armilla, Granada, Spain

E-mail: martarodrigo@ugr.es

1   **Abstract**

2   Oxygen exposure has a large impact on lipid biomarker preservation in surface

3   sediments and may affect the application of organic proxies used for reconstructing past

4   environmental conditions. To determine its effect on long chain alkyl diol and keto-ol based

5   proxies, the distributions of these lipids was studied in nine surface sediments from the

6   Murray Ridge in the Arabian Sea obtained from varying water depths (900 to 3000 m) but in

7   close lateral proximity and, therefore, likely receiving a similar particle flux. Due to

8   substantial differences in bottom water oxygen concentration (<3 to 77 μmol/L) and

9   sedimentation rate, substantial differences exist in the time the biomarker lipids are exposed to

10 oxygen in the sediment. Long chain alkyl diol and keto-ol concentrations in the surface

11 sediments (0-0.5 cm) decreased progressively with increasing oxygen exposure time,

12 suggesting increased oxic degradation. The 1,15-keto-ol/diol ratio (DOXI) increased slightly

13 with oxygen exposure time as diols had apparently slightly higher degradation rates than keto-

14 ols. The ratio of 1,14- vs. 1,13- or 1,15-diols, used as upwelling proxies, did not show

15 substantial changes. However, the C_{30} 1,15-diol exhibited a slightly higher degradation rate

16 than C_{28} and C_{30} 1,13-diols, and thus the Long chain Diol Index (LDI), used as sea surface

17 temperature proxy, showed a negative correlation with the maximum residence time in the

18 oxic zone of the sediment, resulting in ca. 2-3.5 ℃ change, when translated to temperature.

19 The $U^{K'}_{37}$ index did not show significant changes with increasing oxygen exposure. This

20 suggests that oxic degradation may affect temperature reconstructions using the LDI in oxic

21 settings and where oxygen concentrations have varied substantially over time.

22

23 **Keywords:** long chain alkyl diols, keto-ols, LDI, $U^{K'}_{37}$, upwelling indices, DOXI, oxygen

24 minimum zone, Arabian Sea, surface sediments, oxic degradation.

25

1. Introduction

Long chain alkyl diols and keto-ols are structurally related groups of lipids occurring widespread in Quaternary marine and lake sediments (e.g., Versteegh et al., 1997, 2000). These lipids were first discovered in Black Sea sediments by de Leeuw et al. (1981). Commonly occurring long chain alkyl diols found in marine and lake environments are C_{28}-C_{32} 1,13-, 1,14- and 1,15-diols (Versteegh et al., 1997; Rampen et al., 2014a, b). Saturated and mono-unsaturated C_{28} and C_{30} 1,14-diols are produced by *Proboscia* diatoms (Sinninghe Damsté et al., 2003; Rampen et al., 2007) and saturated C_{28}, C_{30} and C_{32} 1,14-diols are synthesized by the marine Dictyochophyte *Apedinella radians* (Rampen et al., 2011). Mono-unsaturated long chain 1,14-alkyl diols have, up to now, only been found in *Proboscia* species, while C_{32} 1,14-diols have only been identified in *Apedinella*. Studies of the descending particle flux in the Arabian Sea confirmed the role of *Proboscia* diatoms as a source for long chain 1,14-alkyl diols in marine sediments, but the importance of *Apedinella* as a source remains uncertain (Rampen et al., 2008, 2011, 2014a). C_{28}-C_{32} long chain 1,13- and 1,15-alkyl diols have been identified in cultures of eustigmatophyte algae (Volkman et al., 1992, 1999; Gelin et al., 1997a; Méjanelle et al., 2003; Shimokwara et al., 2010; Rampen et al., 2014b). However, the role of eustigmatophyte algae as a source in the marine environment is still unclear since there are discrepancies in the long chain alkyl diol composition and distribution between cultures and marine settings (Volkman et al., 1992; Versteegh et al., 1997; Rampen et al., 2012, 2014b).

Different indices based on long chain alkyl diols have been proposed as indicators of upwelling and sea surface temperature (SST) (e.g. Versteegh et al., 1997, 2000; Rampen et al., 2008, 2012; Willmott et al., 2010). The Long chain Diol Index (LDI) is based on the correlation of the fractional abundance of long chain C_{28} 1,13-, C_{30} 1,13- and C_{30} 1,15-alkyl diols with SST (Rampen et al., 2012). Thus far, the LDI has been applied for reconstruction of

51   SST in the mid-latitude regions (Lopes dos Santos et al., 2013; Smith et al., 2013; Rodrigo-

52   Gámiz et al., 2014; Plancq et al., 2015). Upwelling indices are based on the relative

53   abundance of C_{28}-C_{30} 1,14-diols vs. 1,13-diols or C_{30} 1,15-diols (Rampen et al., 2008;

54   Willmott et al., 2010) and have been applied in several oceanic regions, including the Arabian

55   Sea (e.g. Rampen et al., 2008, 2014a; Pancost et al., 2009; Willmott et al., 2010; Lopes dos

56   Santos et al., 2012; Seki et al., 2012). C_{30} and C_{32} keto-ols also occur ubiquitously in marine

57   sediments (e.g., Jiang et al., 1994; Versteegh et al., 1997; Wakeham et al., 2002; Sinninghe

58   Damsté et al., 2003; Rampen et al., 2007; Bogus et al., 2012), and have been identified in a

59   cultured marine eustimatophyte, *Nannochloropsis gaditana,* although in lower amounts than

60   generally found in marine sediments (Méjanelle et al., 2003). Long chain keto-ols have been

61   inferred to be intermediate products of the oxidation of diols and the Diol Oxidation Index

62   (DOXI) has been proposed as an indicator for oxic degradation in the sedimentary record

63   (Ferreira et al., 2001; Versteegh et al., 2010; Bogus et al., 2012). However, the chain length

64   distributions and distributions of positional isomers for long chain alkyl diols and the

65   corresponding keto-ols differ (Versteegh et al., 1997), casting some doubts on the occurrence

66   of this oxidation process. Another suggestion for the origin of keto-ols is that they may be

67   produced by an as yet unknown biological source (Versteegh et al., 1997).

68   Like many other organic proxies, uncertainties remain in the application of long chain

69   alkyl diols as palaeoclimate reconstruction tools. Apart from the fact that the biological source

70   of 1,13- and 1,15-diols in the marine environment is still unknown, a variety of environmental

71   factors other than temperature (e.g. salinity, nutrient availability) could have an impact on

72   these proxies. Importantly, diagenesis can have a substantial effect on the abundance and

73   distributions of biomarker lipids (e.g. Arzayus and Canuel, 2004; Peters et al., 2005 and

74   references cited therein). One important factor affecting lipid distributions and preservation is

75   oxic degradation (e.g., Sun and Wakeham, 1994; Hoefs et al., 1998, 2002; Sinninghe Damsté

76 et al., 2002; Prahl et al., 2003; Rontani et al., 2009, 2013), particularly oxygen exposure time

77 (Hartnett et al., 1998; Hedges et al., 1999). For example, it has been shown that the $U^{K'}_{37}$-SST

78 proxy based on alkenones may be altered after long term exposure to oxygen (Hoefs et al.,

79 1998, 2002; Gong and Hollander, 1999; Prahl et al., 2003; Rontani et al., 2009, 2013). The

80 effect of degradation on long chain alkyl diol distributions, and the proxies based on these

81 components, is, however, still not clear (Ferreira et al., 2001; Versteegh et al., 2010; Bogus et

82 al., 2012).

83   In this study we investigated the impact of oxic degradation on long chain alkyl diol

84 and long chain keto-ol (referred as diols and keto-ols hereafter) concentrations by analyzing

85 nine surface sediments from the Murray Ridge in the Arabian Sea. Previous studies have

86 shown that this submarine high in the northern Arabian Sea provides an excellent location to

87 study the effect of oxygen degradation on lipid distributions (Sinninghe Damsté et al., 2002;

88 Schouten et al., 2012; Lengger et al., 2012, 2014). The Murray Ridge protrudes into one of the

89 largest oxygen minimum zones (OMZ) presently found in the oceans, with molecular oxygen

90 (O_2) concentrations varying from minima of 0.1-1.0 μmol/L to maxima of ~22 μmol/L along

91 the OMZ (Olson et al., 1993; Paulmier and Ruiz-Pino, 2009). Below the OMZ, oxygen

92 concentrations substantially increase by up to ca. 80 μmol/L, providing a strong gradient in

93 bottom water oxygen concentrations. The set of surface sediments studied are in close lateral

94 proximity, and hence likely receive a similar flux of pelagic organic matter, but have

95 contrasting bottom water oxygen concentrations, thus allowing to constrain the effect of oxic

96 degradation on organic matter and biomarkers (cf. Sinninghe Damsté et al., 2002; Schouten et

97 al., 2012; Bogus et al., 2012; Lengger et al., 2012, 2014). Here, we have studied the effect of

98 the oxic degradation on concentrations of diols and related proxies (i.e. LDI, upwelling,

99 DOXI). We compared our results with those of alkenone concentrations and the $U^{K'}_{37}$ index.

100 Furthermore, we evaluated the possible origin of keto-ols as oxic transformation products of

101 diols.

102

103 **2. Material and methods**

104 *2.1. Sampling*

105   Surface sediments (0-0.5 cm sediment depth) were obtained in the Northern Arabian

106 Sea along a depth transect on the Murray Ridge during the PASOM cruise (64PE301) in

107 January 2009 with the *R/V Pelagia* (Fig. 1a; Koho et al., 2013; Lengger et al., 2014).

108 Sediments were stored in geochemical bags and frozen immediately at -80°C on board and

109 transported and subsequently stored at -20°C. A total of nine box cores were taken at different

110 water depths, ranging from 885 to 3010 m, with bottom water oxygen concentrations (BWO)

111 ranging from <3 to 77 µmol/L, i.e. three within the OMZ (P900, P1000, P1200), two in the

112 suboxic zone just below the OMZ (P1300, P1500) and four in the oxic zone well below the

113 OMZ (P1800, P2000, P2500, P3000) (Fig. 1b). Oxygen concentrations of the water column,

114 oxygen penetration depths, total organic carbon content and sedimentation rates have been

115 previously reported by Koho et al. (2013) and Lengger et al. (2014).

116

117 *2.2. Extraction*

118   Prior to analysis, surface sediments were freeze-dried and homogenized in an agate

119 mortar. After addition of pre-extracted diatomaceous earth, aliquots (1-2 g) of surface

120 sediments were extracted in an Accelerated Solvent Extractor 350 (ASE 350, DIONEX) using

121 a solvent mixture of 9:1 (v:v) dichloromethane (DCM) to methanol (MeOH) at 100 ºC and 7.6

122 x 10^6 Pa. The solvent was reduced by TurboVap LV Caliper. Extracts were dried over a

123 pipette column containing Na_2SO_4 and concentrated under a stream of N_2.

124   Two internal standards were added to the total lipid extracts (TLEs) prior to column

125   chromatography separation, i.e. 3.2 µg 10-nonadecanone for alkenone quantitation and 0.258

126   µg C_{22} 7,16-diol for quantitation of diols. Apolar, ketone and polar fractions were obtained by

127   column chromatography using a Pasteur pipette filled with Al_2O_3 (activated for 2 h at 150 ºC)

128   using respectively 9:1 (v:v) hexane:DCM, 1:1 (v:v) hexane:DCM, and 1:1 (v:v) MeOH:DCM

129   as the eluents.

130

131   *2.2.1. GC analysis*

132   The ketone fractions were dried under N_2 and re-dissolved in an appropriate volume

133   (50-400 µl) of hexane. Analysis of the alkenones was performed in duplicate on an Hewlett

134   Packard 6890 Gas Chromatograph (GC) using a 50-m CP Sil-5 column (0.32-mm diameter,

135   film thickness of 0.12 µm), equipped with flame ionization detector and helium as the carrier

136   gas. The temperature of the oven was initially 70°C and increased with a rate of 20°C per min

137   to 200°C and subsequently with a rate of 3°C per min to 320°C, at which it was held for 25

138   min. Alkenone abundances were determined by integration of relevant peak areas and the

139   internal standard (10-nonadecanone).

140   The $U^{K'}_{37}$ index (Eq. 1) was calculated according to the equation by Prahl and

141   Wakeham (1987):

142

143    $$U^{K'}_{37} = \frac{[C_{37:2}]}{[C_{37:2}]+[C_{37:3}]} \hspace{4cm} (1)$$

144

145        $U^{K'}_{37}$ values were converted to SSTs using the global core top calibration of Müller et

146   al. (1998):

147

148    $$U^{K'}_{37} = 0.033 \times SST + 0.044 \hspace{4cm} (2)$$

149

150   *2.2.2. GC-MS analysis*

151   The polar fractions were dried under N_2 and silylated by adding 15 µl N,O-

152   bis(trimethylsilyl)trifluoroacetamide (BSTFA) and pyridine and heating in an oven at 60°C

153   for 20 min. Diol and keto-ol distributions were analyzed in duplicate using a Thermo Finnigan

154   Trace Gas Chromatograph (GC) Ultra coupled to a Thermo Finnigan DSQ mass spectrometer

155   (MS). A 25-m CP Sil-5 fused silica capillary column was used (25 m x 0.32 mm; film

156   thickness = 0.12 µm) with helium as the carrier gas. The column was directly inserted into the

157   electron impact ion source of the DSQ quadrupole MS with an ionization energy of 70 eV.

158   Samples were dissolved in 30-500 µl ethyl acetate and injected at 70°C. The oven was

159   programmed to increase first at a rate of 20°C per min to 130°C, and then at a rate of 4°C per

160   min to the final temperature of 320°C (held 25 min). Various diols and the C_{22} 7,16-diol

161   standard were quantified using single ion monitoring (SIM) of *m/z* 299, 313, 327, 341, 369

162   and 187, respectively, and keto-ols were quantified using SIM of *m/z* 300, 314 and 328. A

163   correction factor for quantifying diol and keto-ol concentrations was applied as follows: the

164   mass fragments of the diols contributed on average 12.9% to the total ion counts, that of the

165   C_{22} 7,16-diol standard contributed on average 22% to the total ion counts and that of the keto-

166   ols contributed on average 9% to the total ion counts.

167   The Long chain Diol Index (LDI) was calculated and converted to SST following

168   Rampen et al. (2012):

169

170    $$LDI = \frac{[C_{30}1,15-diol]}{[C_{28}+C_{30}1,13-diol]+[C_{30}1,15-diol]} \tag{3}$$

171

172    $$LDI = 0.033 \times SST + 0.095 \tag{4}$$

173

174   The following two upwelling indices (Diol Index 1 and 2 referred as 1,15 upw and

175   1,13 upw, respectively, hereafter) were calculated according to Rampen et al. (2008) and

176   Willmott et al. (2010), respectively:

177

178     $1,15\ upw = \frac{[C_{28}+C_{30}\,1,14-diol]}{[C_{28}+C_{30}\,1,14-diol]+[C_{30}\,1,15-diol]}$ (5)

179

180     $1,13\ upw = \frac{[C_{28}+C_{30}\,1,14-diol]}{[C_{28}+C_{30}\,1,14-diol]+[C_{28}+C_{30}\,1,13-diol]}$ (6)

181

182   The Diol Oxidation Index (DOXI) was calculated according to Ferreira et al. (2001)

183   for diols and keto-ols with identical carbon chain-lengths and carbon position of the mid-

184   chain functional groups:

185

186     $DOXI = \frac{[keto-ol]}{[keto-ol]+[diol]}$ (7)

187

188   **3. Results**

189   *3.1. Bulk parameters*

190   The nine sampling stations along the Murray Ridge show an increase in bottom water

191   oxygen concentrations (from 3 to 77 μmol/L; Fig. 1b) and oxygen penetration depths, and a

192   decrease in sedimentation rates with increasing water depth (cf. Koho et al., 2013; Lengger et

193   al., 2014). Increasing oxygen penetration depth and decreasing sedimentation rate lead to an

194   increase in the maximum residence time the organic matter spends in the oxic zone (t_{OZ},

195   calculated from the oxygen penetration depth and the sediment accumulation rate; see

196   Lengger et al., 2014 for details). Concentrations of organic carbon (C_{org}) decreased

197   progressively with increasing water depth or increasing t_{OZ} (from 60 to 10 mg/g sediment dry

198   weight, referred as mg/g hereafter) (Fig. 2a) (data from Lengger et al., 2014). This indicates

199   that the surface sediments show an increasing degradation of organic matter as a result of the

200   increasing residence time in the oxic zone of the sediment (Lengger et al., 2012, 2014; Koho

201   et al., 2013).

202

203   *3.2. Diols and keto-ols*

204   The surface sediments contained a range of diols and keto-ols. Diols consisted of C_{28}-

205   C_{34} 1,13-, 1,14- and 1,15-isomers, dominated by the C_{30} 1,14-diol (Supplementary Table S1).

206   The keto-ols consisted of C_{30}-C_{34} homologues with the keto group at the 15 position

207   (Supplementary Table S1), and low abundance of the C_{30} 1,14-keto-ol (data not shown). The

208   concentrations of diols used for the LDI in the surface sediments decreased strongly with

209   water depth from 4.3, 0.14 and 0.11 µg/g to 0.15 and 0.01 µg/g for C_{30} 1,15-, and C_{30}-C_{28}

210   1,13-diols, respectively, with the largest decrease in the suboxic zone (Fig. 2c). The

211   concentration of the other abundant 1,15-diol, the C_{32} 1,15-diol, decreased with water depth

212   from 1.28 to 0.04 µg/g (Fig. 2b). The 1,14-diols shows a similar pattern as the 1,13 and 1,15-

213   diols, i.e. C_{28} and C_{30} 1,14-diols decreased from 4.5 and 4.1 µg/g, respectively, to ca. 0.2 µg/g

214   (Fig. 2b). The concentration of the mono-unsaturated C_{28} 1,14-diol decreased from 0.22 to

215   0.01 µg/g, while that of the mono-unsaturated C_{30} 1,14-diol decreased even more sharply from

216   2.90 up to 0.01 µg/g (Fig. 2b). Individual concentrations of C_{30}, C_{32} and C_{34} 1,15-keto-ols

217   ranged between 2.3-0.17, 3.3-0.29, and 0.46-0.03 µg/g, respectively, and also strongly

218   decreased with increasing water depth (Fig. 2e).

219   Calculation of the different indices based on the various diol isomers shows different

220   patterns. The LDI values ranged between 0.95 and 0.89, with a minimum value of 0.84 at

221   1970 m water depth, showing a distinct decrease with increasing water depth from the anoxic

222   to the oxic zone (Fig. 3a). The upwelling indices showed minor variations with 1,14- vs. 1,15-

223 diol upwelling index varying between 0.67 and 0.74 with a slight increase with water depth

224 (Fig. 3b), while the 1,14- vs. 1,13-diol upwelling index varied between 0.97 and 0.93 with a

225 slight decrease with increasing water depth (Fig. 3b). DOXI values varied between 0.24-0.37,

226 0.73-0.81, and 0.76-0.89 for the C_{30}, C_{32}, and C_{34} keto-ol/diol ratio based on 1,15 isomers,

227 respectively, with no distinct trends (Fig. 3c). The C_{28} 1,15-keto-ol was not detected and

228 therefore the C_{28} based DOXI value was 0.

229

230 *3.3. Alkenones*

231   The concentration of the individual C_{37} alkenones in surface sediments generally

232 decreased with increasing water depth (Supplementary Table S1), with concentrations

233 decreasing from 12.9 and 0.46 µg/g to 0.76 and 0.03 µg/g for the $C_{37:2}$ and $C_{37:3}$ alkenones,

234 respectively (Fig. 2f). Values for the $U^{K'}_{37}$ index varied between 0.97 and 0.95 with no

235 particular trend (Fig. 3a).

236

237 **4. Discussion**

238 *4.1. Impact of sedimentary oxic degradation on diol and alkenone concentrations*

239   In the surface sediments studied here, the 1,14-diols are more abundant than the 1,15-

240 diols and 1,13-diols (Fig. 2d), suggesting that *Proboscia* diatoms (Sinninghe Damsté et al.,

241 2003; Rampen et al., 2007) are an abundant source of diols in the Arabian Sea. This is in

242 agreement with previous studies in this area showing high abundances of these lipids with the

243 highest annual fluxes for the 1,14-diols compared to other diol isomers (Rampen et al., 2007,

244 2008). Wakeham et al. (2002) reported the dominance of C_{30} 1,15-diols over 1,13- and 1,15-

245 diols in descending particles trapped at shallow and middle depth (~500 and 1460 m,

246 respectively) in the Arabian Sea water column, which is consistent with the distribution

247 observed in this study. In general, all diols showed similar trends, i.e. a strong decrease in

248   concentration with increasing water depth and thus increasing oxygen content in the bottom

249   and pore waters of the sediment and increasing residence time in the oxic part of the sediment

250   (Figs. 2b-c). This suggests that all diols are affected by oxic degradation, in agreement with

251   earlier studies (e.g., Hoefs et al., 2002; Sinninghe Damsté et al., 2002). Indeed, 1,13-, 1,14-

252   and 1,15-diol concentrations revealed a significant negative correlation with t_{OZ} (e.g. Figs. 4b-

253   c, f). However, the slopes of the equations describing these linear correlations differ between

254   the various diols, with some diols (e.g. the C_{30} 1,13-diol) having a smaller slope than other

255   diols, suggesting lower degradation rates. Different degradation rates have been described for

256   different lipid biomarker classes and even between structurally similar biomarker lipids such

257   as di- and tri-unsaturated alkenones (e.g., Hoefs et al., 1998, 2002; Gong and Hollander, 1999;

258   Sinninghe Damsté et al., 2002; Versteegh et al., 2010).

259   To compare the extent of oxic degradation for the different diols, we calculated the

260   relative preservation efficiency (RPE; in %). This was calculated by taking the average of the

261   concentrations of a specific diol in the three surface sediments with the highest t_{OZ} (i.e.

262   stations P2000, P2500, and P3000 from the oxic zone below the OMZ; Fig. 1b) and compare

263   this with that in the shallowest surface sediment with the lowest t_{OZ}, i.e. from within the OMZ

264   (i.e. station P900 within the core of the OMZ; Fig. 1b) (Fig. 5a). This shows that increased

265   oxygen exposure time leads to the degradation of 89-96% of the diols. Values of the RPE

266   show differences between positional isomers, i.e. the 1,13-diols show the best preservation (~

267   11 %), followed by 1,14-diols (~ 6 %) and finally 1,15-diols (~ 4 %) but is independent of

268   chain length of the diols (Fig. 5a).

269   The difference in the extent of degradation of the various diols could be related to the

270   different biological sources of diols, i.e. 1,14-diols are mainly synthesized by *Proboscia*

271   diatoms (Sinninghe Damsté et al., 2003; Rampen et al., 2007), while 1,15- and 1,13-diols are

272   produced by eustigmatophyte algae (Volkman et al., 1992, 1999). However, we observed a

273 rather large difference in RPE for 1,15- and 1,13-diols, which in principle are presumed to be

274 derived from the same biological source (Rampen et al., 2012). Structurally, there seems no

275 reason for such a significant difference in RPE. This may imply a different physical protection

276 of the diol isomers, e.g. adsorbed to different ballast minerals (Hedges et al., 2001; Armstrong

277 et al., 2002), which would also imply different sources for these diols. Alternatively, the

278 different degradation rates may indicate that diols do not only occur as free-lipids but also in a

279 bound form (Gelin et al., 1997a; Grossi et al., 2001; Shimokwara et al., 2010; Rampen et al.,

280 2014a), which may cause a release of diols by hydrolysis during early diagenesis. If, for

281 example, 1,13-diols are more abundant in a bound form than in the free form, then the release

282 of these bound diols during diagenesis could lead to an apparent higher RPE for 1,13-diols.

283   Alkenone concentrations also dropped substantially with increasing water depth and

284 t_{OZ} (Figs. 2f, 4h-i), indicating that they are affected by oxic degradation as well. They showed

285 similar values for RPE, i.e. 10-12 % (Fig. 5b) as the 1,13-diols (~ 11 %), but higher than those

286 for 1,14- and 1,15-diols. There is a slight difference in RPE for both alkenones, i.e. 12 % for

287 $C_{37:3}$ and 10.6 % for $C_{37:2}$ (Fig. 5b), but this is mainly caused by the sediment of station P900

288 (at 885 m water depth), which seems somewhat anomalous with respect to the concentration

289 of the $C_{37:3}$ alkenone. If the alkenone concentrations in the sediment of station P1000 (at 1013

290 m water depth, still within the OMZ, Fig. 1b) are used, then RPEs of both alkenones are

291 relatively similar, in agreement with previous observations in this region (Sinninghe Damsté

292 et al., 2002).

293

294 *4.2. Impact of oxic degradation on paleoenvironmental proxies*

295   Because the 1,13-diols are slightly better preserved (Fig. 5a) than 1,15-diols, the LDI

296 decreases from 0.94 to 0.85 with increasing water depth (Fig. 3a). Moreover, a linear negative

297 correlation of LDI with t_{OZ} is observed ($R^2 = 0.86$; Fig. 4a), suggesting that the LDI is

298   affected by oxic degradation. Low abundances of biomarkers may lead to analytical biases as

299   has been observed with the $U^{K'}_{37}$ (Villanueva and Grimalt, 1997). However, a dilution test

300   (data not shown) showed that the changes in LDI values are not because of analytical artifacts

301   due to the low amounts of diols present in the oxidized sediments. When translated to SST,

302   the LDI variations correspond to a change from 25.5 to 24 ºC, with a minimum of 23 ºC at ca.

303   2000 m water depth in the oxic zone. This change of ca. 1.5-2.5 ºC is similar to, or even

304   exceeds if we consider the somewhat anomalous data point at ca. 2000 m water depth, the

305   calibration error of this proxy (2 °C; Rampen et al., 2012), suggesting that this SST proxy can

306   be affected by oxic degradation.

307   For comparison, we also analyzed the established SST proxy based on alkenones, the

308    $U^{K'}_{37}$ index. A previous study of alkenones in sediments from the Murray Ridge in the

309   Arabian Sea documented no significant degradation effect (Sinninghe Damsté et al., 2002).

310   Indeed, $U^{K'}_{37}$ values showed, with the exception of the shallowest sediment, no significant

311   variation with increasing water depth (Fig. 3a) and thus with increasing residence time in the

312   oxic zone of the sediment (Fig. 4g). The mean $U^{K'}_{37}$ value of 0.96 corresponds to 27.6 ºC

313   when translated to SST (Fig. 3a). This $U^{K'}_{37}$-estimated SSTs are in good agreement with

314   present annual mean SST in the Arabian Sea (ca. 27 ºC, World Ocean Atlas 09 database;

315   Locarnini et al., 2010). Another paleotemperature proxy, the TEX_{86}, was previously measured

316   in the same set of surface sediments as studied here and showed differences in derived SST

317   with increasing water depth and t_{OZ}, corresponding to higher values of up to 3 ºC (Lengger et

318   al., 2014). Although several hypotheses were put forward, the reasons for this change in

319   TEX_{86} were not clear.

320   The upwelling indices based on diols showed contrasting patterns compared to each

321   other as a result of the different degradation rates of 1,14-diols vs. 1,15- and 1,13-diols (Figs.

322   2b-c). The upwelling index based on 1,14- vs. 1,15-diols (Rampen et al., 2008), did not

323   correlate with t_{OZ} (Fig. 4d), but an apparent correlation is observed for the upwelling index

324   based on 1,14- vs. 1,13-diols (Willmott et al., 2010) (Fig. 4e). Indeed, the latter index displays

325   a small, but significant, decreasing trend with increasing water depth (Fig. 3b). However,

326   these changes (< 0.05 units) are relatively small compared to changes documented in Arabian

327   Sea sediment trap records (> 0.05 units; Rampen et al., 2007) and in globally distributed

328   surface sediments (Rampen et al., 2014a).

329   Thus, among the diol based proxies tested in this study the LDI seems to be most

330   affected by preferential oxic degradation in the Arabian Sea. These results indicate that this

331   effect has to be taken into consideration, especially when paleotemperature reconstructions

332   are performed in sediments where bottom water oxygen concentrations or oxygen penetration

333   depths have varied substantially over time.

334

335   *4.3. Keto-ols: intermediate products or biologically sourced?*

336   Keto-ols have been described as oxic transformation products of diols (e.g. Jiang et al.,

337   1994; Ferreira et al., 2001; Versteegh et al., 1997, 2010). Keto-ol concentrations in an

338   unoxidised sapropel layer in the eastern Mediterranean were lower than at the base of the

339   oxidized sapropel (Ferreira et al., 2001), suggesting that keto-ols are formed by oxidation of

340   diols. Based on these observations, the DOXI was proposed as a potential indicator for

341   paleoxicity in the water column (Ferreira et al., 2001). In the Arabian Sea surface sediments,

342   one might expect higher abundances of keto-ols relative to diols in sediments with a higher

343   exposure time to oxygen. The C_{30}-C_{34} 1,15-keto-ol concentrations showed a strong decrease

344   with increasing water depth, similar to that of the diols (Fig. 2e), and remained always lower

345   than the corresponding 1,15-diols (Figs. 2c-e). However, the C_{30}-C_{34} keto-ols were apparently

346   slightly better preserved than the corresponding diols, i.e. the RPE of the 1,15-keto-ols (~ 8%)

347   is slightly higher than that of the 1,15-diols (~ 4 %) (Fig. 5c). Indeed, the C_{30}, C_{32} and C_{34}

348   1,15 DOXI ratios are slightly higher in the oxic zone compared to the anoxic zone but the

349   differences are relatively minor (Fig. 3c). This is in contrast with results of a similar study

350   along the OMZ transect on the Pakistan continental margin, which showed a much stronger

351   increase of the C_{30} 1,15 DOXI ratio with increasing oxygen concentrations (Bogus et al.,

352   2012). The reason for the reduced DOXI values increase in the Arabian Sea sediments might

353   be the much lower bottom water oxygen concentrations (45-77 μmol/L) and oxygen

354   penetration depths (6-19 mm; Lengger et al., 2014) versus those at the Pakistan margin (220

355   μmol/L and 25 mm, respectively; Bogus et al., 2012). Indeed, Bogus et al. (2012) observed a

356   much smaller increase in DOXI values in sediments with bottom water oxygen concentrations

357   and oxygen penetration depths comparable to the Arabian Sea sediments studied here. This

358   suggests that DOXI values only substantially increase after a long-term exposure to high

359   oxygen concentrations.

360   Interestingly, the keto-ols are already observed in sediments from within the OMZ.

361   This may suggest that they were already formed in the upper part of the oxic water column

362   overlying the OMZ. This is supported by sediment trap material collected in and below the

363   OMZ of the Arabian Sea, which contained both C_{30} 1,15-keto-ols and saturated and mono-

364   unsaturated C_{30} 1,14-keto-ols (Rampen et al., 2007). However, a previous study of biomarkers

365   in sedimenting particles in and below the OMZ in the Arabian Sea documented that the degree

366   of degradation of biomarkers in the water column is insignificant relative to that in the surface

367   sediment (Wakeham et al., 2002) due to relatively short oxygen exposure time during sinking

368   of the particles. Therefore, it is not expected that keto-ols are formed solely by oxic

369   transformation in the water column during the vertical transport to the sea floor.

370   Another possibility is that keto-ols are synthesized by the algae themselves, i.e.

371   eustigmatophytes or as yet unknown algae (Versteegh et al., 1997; Méjanelle et al., 2003).

372   Méjanelle et al. (2003) identified C_{28}-C_{36} diols and C_{30}-C_{32} keto-ols with the C_{32} keto-ol

373 slightly dominating over the other homologues in a marine eustigmatophyte, *Nannochloropsis*

374 *gaditana*. In addition, only the 1,15-isomer was observed for the C_{32} keto-ol, while 1,13-

375 isomer together with the 1,15-isomer in minor amounts were observed for the C_{30} keto-ol

376 (Méjanelle et al., 2003). In the Arabian Sea surface sediments we identified C_{30} to C_{34} keto-

377 ols with a predominance of 1,15- over 1,13-isomers, while 1,14-isomers were below detection

378 limit (data not shown). Similar to what has been observed in *Nannochloropsis gaditana*, the

379 C_{32} 1,15 keto-ol was in slightly highest abundance (Fig. 2e). Nevertheless, keto-ols and diols

380 are within the same order of magnitude in marine sediments whereas a marked disproportion

381 is observed in the algal cultures. Further evidence for a biological imprint on the distribution

382 of keto-ols comes from the observation that DOXI values differ substantially between carbon

383 chain lengths (Fig. 3c), suggesting some initial biological control for either diols or keto-ols,

384 possibly eustigmatophytes and/or yet additional unidentified algae, and the contribution, at

385 least to some extent, to the sediment.

386

387 **5. Conclusions**

388 In order to determine the effect of oxic degradation on diols and keto-ols, we analyzed

389 nine surface sediments in the Arabian Sea deposited under contrasting bottom water oxygen

390 concentrations. In general, the concentrations of all diols showed a strong decrease with

391 increasing oxygen concentration and increasing residence time in oxic zone of the sediment.

392 A higher degradation rate was found for 1,15-diols, followed by 1,14-diols and 1,13-diols.

393 The LDI showed a decrease from 0.95 to 0.88 with increasing water depth, corresponding to

394 ca. 2-3.5 ºC when translated to SST. For comparison with an established SST proxy, we have

395 also analyzed alkenone concentrations and the $U^{K'}_{37}$ index, obtaining that individual alkenones

396 were affected by oxic degradation as well, but no significant changes are observed in the $U^{K'}_{37}$

397 index. Therefore, care has to be taken when the LDI is applied as SST proxy in sediments

underlying OMZs or where bottom water oxygen concentrations have varied substantially over time. In contrast, upwelling indices based on the ratios of 1,14-diols versus 1,13- or 1,15-diols showed relatively small changes, indicating that these proxies are not substantially affected by variations in bottom water oxygen conditions. C_{30}-C_{34} keto-ol concentrations are apparently slightly less degraded with increasing oxygen exposure time compared to diols and DOXI values show a small increase between the anoxic to the oxic zone. Possibly, longer exposure times to oxygen are needed in order to substantially increase DOXI values.

Data from this publication are archived in the data centre "Pangaea" (www.Pangaea.de).

References

Armstrong, R.A., Lee, C., Hedges, J.I., Honjo, S., Wakeham, S.G., 2002. A new, mechanistic model for organic carbon fluxes in the ocean based on the quantitative association of POC with ballast minerals. Deep-Sea Research Part II 49, 219-236.

Arzayus, K.M., Canuel, E.A., 2004. Organic matter degradation in sediments of the York River estuary: Effects of biological vs. physical mixing. Geochimica et Cosmochimica Acta 69, 455-463.

Bogus, K.A., Zonneveld, K.A.F., Fischer, D., Kasten, S., Bohrmann, G., Versteegh, G.J.M., 2012. The effect of meter-scale lateral oxygen gradients at the sediment-water interface on selected organic matter based alteration, productivity and temperature proxies. Biogeosciences 9, 1553-1570.

De Leeuw, J.W., Rijpstra, W.I.C., Schenck, P.A., 1981. The occurrence and identification of C_{30}, C_{31} and C_{32} alkan-1,15-diols and alkan-15-one-1-ols in Unit I and Unit II Black Sea sediments. Geochimica et Cosmochimica Acta 45, 2281-2285.

Ferreira, A.M., Miranda, A., Caetano, M., Baas, M., Vale, C., Sinninghe Damsté, J.S., 2001. Formation of mid-chain alkane keto-ols by post-depositional oxidation of mid-chain diols in Mediterranean sapropels. Organic Geochemistry 32, 271-276.

Gelin, F., Boogers, I., Noordeloos, A.A.M., Sinninghe Damsté, J.S., Riegman, R., de Leeuw, J.W., 1997a. Resistant biomaeromolecules in maline microalgae of the classes Eustigmatophyceae and Chlorophyceae: Geochemical implications. Organic Geochemistry 26, 659-675.

Gong, C., Hollander, D.J., 1999. Evidence for differential degradation of alkenones under contrasting bottom water oxygen conditions: Implications for paleotemperature reconstruction. Geochimica et Cosmochimica Acta 63, 405-411.

Grossi, V., Blokker, P., Sinninghe Damsté, J.S., 2001. Anaerobic biodegradation of lipids of the marine microalga *Nannochloropsis salina*. Organic Geochemistry 32, 795-808.

Hartnett, H.E., Keil, R.G., Hedges, J.I., Devol, A.H., 1998. Influence of oxygen exposure time on organic carbon preservation in continental margin sediments. Nature 391, 572-573.

Hedges, J.I., Hu, F.S., Devol, A.H., Hartnett, H.E., Tsamakis, E., Keil, R.G., 1999. Sedimentary organic matter preservation: A test for selective degradation under oxic conditions. American Journal of Science 299, 529-555.

Hedges, J.I, Baldock, J.A., Gélinas, Y., Lee, C., Peterson, M., Wakeham, S.G., 2001. Evidence for non-selective preservation of organic matter in sinking marine particles. Nature 409, 801-804.

Hoefs, M.J.L., Versteegh, G.J.M., Rijpstra, W.I.C., de Leeuw, J.W., Sinninghe Damsté, J.S., 1998. Postdepositional oxic degradation of alkenones: Implications for the measurement of palaeo sea surface temperatures. Paleoceanography 13, 42-49.

Hoefs, M.J.L., Rijpstra, I.C., Sinninghe Damsté, J.S., 2002. The influence of oxic degradation on the sedimentary biomarker record I: Evidence from Madeira Abyssal Plain turbidites. Geochimica et Cosmochimica Acta 66, 2719-2735.

461   Jiang, S.C., O'Leary, T., Volkman, J.K., Zhang, H.Z., Jia, R.F., Yu, S.H., Wang, Y., Luan, Z.F., Sun,

462   Z.Q., Jiang, R.H., 1994. Origins and simulated thermal alteration of sterols and keto-alcohols in

463   deep-sea marine sediments of the Okinawa Trough. Organic Geochemistry 21, 415-422.

464   Koho, K.A., Nierop, K.G.J., Moodley, L., Middelburg, J.J., Pozzato, L., Soetaert, K., van der Plicht, J.,

465   Reichart, G.-J., 2013. Microbial bioavailability regulates organic matter preservation in marine

466   sediments. Biogeosciences 10, 1131-1141.

467   Lengger, S.K., Hopmans, E.C., Reichart, G.-J., van Nierop, K.G.J., Sinninghe Damsté, J.S., Schouten,

468   S., 2012. Intact polar and core glycerol dibiphytanyl glycerol tetraether lipids in the Arabian Sea

469   oxygen minimum zone. Part II: Selective preservation and degradation in sediments and

470   consequences for the TEX_{86}. Geochimica et Cosmochimica Acta 98, 244-258.

471   Lengger, S.K., Hopmans, E.C., Sinninghe Damsté, J.S., Schouten, S., 2014. Impact of sedimentary

472   degradation and deep water column production on GDGT abundance and distribution in surface

473   sediments in the Arabian Sea: Implications for the TEX_{86} paleothermometer. Geochimica et

474   Cosmochimica Acta 142, 386-399.

475   Locarnini, R.A., Mishonov A.V., Antonov, J.I., Boyer, T.P., Garcia, H.E., Baranova, O.K., Zweng,

476   M.M., Johnson, D.R., 2010. World Ocean Atlas 2009: Volume 1: Temperature, In: Levitus, S.

477   (Ed.), NOAA Atlas NESDIS 68. U.S. Government Printing Office, Washington, D.C., pp. 184.

478   Lopes dos Santos, R.A., Wilkins, D., de Deckker, P., Schouten, S., 2012. Late Quaternary productivity

479   changes from offshore Southeastern Australia: a biomarker approach. Palaeogeography,

480   Palaeoclimatology, Palaeoecology 363-364, 48-56.

481   Lopes dos Santos, R. A., Spooner, M. I., Barrows, T. T., De Deckker, P., Sinninghe Damsté, J. S.,

482   Schouten, S., 2013. Comparison of organic ($U^{K'}_{37}$, TEX^{H}_{86}, LDI) and faunal proxies (foraminiferal

483   assemblages) for reconstruction of late Quaternary sea-surface temperature variability from

484   offshore southeastern Australia. Paleoceanography 28, 377-387.

485   Méjanelle, L., Sanchez-Gargallo, A., Bentaleb, I., Grimalt, J.O., 2003. Long chain n-alkyl diols,

486   hydroxy ketones and sterols in a marine eustigmatophyte, *Nannochloropsis gaditana*, and in

487   *Brachionus plicatilis* feeding on the algae. Organic Geochemistry 34, 527-538.

488   Müller, P.J., Kirst, G., Ruhland, G., von Storch, I., Rossell-Melé, A., 1998. Calibration of alkenone

489   paleotemperature index $U^{K'}_{37}$ based on core tops from the eastern South Atlantic and the global

490   ocean (60ºN–60ºS). Geochimica et Cosmochimica Acta 62, 1757-1771.

491   Olson, D. B., Hitchcock, G. L., Fine, R. A., Warren B. A., 1993. Maintenance of the low-oxygen layer

492   in the central Arabian Sea. Deep-Sea Research Part II 40, 673-685.

493   Pancost, R.D., Boot, C.S., Aloisi, G., Maslin, M., Bickers, C., Ettwein, V., Bale, N., Handley, L.,

494   2009. Organic geochemical changes in Pliocene sediments of ODP Site 1083 (Benguela

495   Upwelling System). Palaeogeography, Palaeoclimatology, Palaeoecology 280, 119-131.

496   Paulmier, A., Ruiz-Pino D., 2009. Oxygen minimum zones (OMZs) in the modern ocean. Progress in

497   Oceanography 80, 113-128.

Peters, K.E., Walters, C.C., Moldowan, J.M., 2005. The Biomarker Guide, 2nd ed. Cambridge University Press, Cambridge, UK, New York.

Plancq, J., Grossi, V., Pitteta, B., Huguet, C., Rosell-Melé, A., Mattioli, E., 2015. Multi-proxy constraints on sapropel formation during the late Pliocene of central Mediterranean (southwest Sicily). Earth and Planetary Science Letters 420, 30-44.

Prahl, F.G., Wakeham, S.G., 1987. Calibration of unsaturation patterns in long-chain ketone compositions for palaeotemperature assessment. Nature 330, 367-369.

Prahl, F.G., de Cowie, G.L., de Lange, G.J., Sparrow, M.A., 2003. Selective organic matter preservation in "burn-down" turbidites on the Madeira Abyssal Plain. Paleoceanography 18, 1052.

Rampen, S.W., Schouten, S., Wakeham, S.G., Sinninghe Damsté, J.S., 2007. Seasonal and spatial variation in the sources and fluxes of long chain diols and mid-chain hydroxy methyl alkanoates in the Arabian Sea. Organic Geochemistry 38, 165-179.

Rampen, S.W., Schouten, S., Koning, E., Brummer, G.-J.A., Sinninghe Damsté, J.S., 2008. A 90 kyr upwelling record from the northwestern Indian Ocean using a novel long-chain diol index. Earth and Planetary Science Letters 276, 207-213.

Rampen, S.W., Schouten, S., Sinninghe Damsté, J.S., 2011. Occurrence of long chain 1,14 diols in *Apedinella radians*. Organic Geochemistry 42, 572-574.

Rampen, S.W., Willmott, V., Kim, J.-H., Uliana, E., Mollenhauer, G., Schefuß, E., Sinninghe Damsté, J.S., Schouten, S., 2012. Long chain 1,13- and 1,15-diols as a potential proxy for palaeotemperature reconstruction. Geochimica et Cosmochimica Acta 84, 204-216.

Rampen, S.W., Willmott, V., Kim, J.-H., Rodrigo-Gámiz, M., Uliana, E., Mollenhauer, G., Schefuß, E., Sinninghe Damsté, J. S., Schouten, S., 2014a. Evaluation of long chain 1,14-diols in marine sediments as indicators for upwelling and temperature. Organic Geochemistry 76, 39-47.

Rampen, S.W., Datema, M., Rodrigo-Gámiz, M., Schouten, S., Reichart, G.-J., Sinninghe Damsté, J.S., 2014b. Sources and proxy potential of long chain alkyl diols in lacustrine environments. Geochimica et Cosmochimica Acta 144, 59-71.

Rodrigo-Gámiz, M., Martínez-Ruiz, F., Rampen, S. W., Schouten, S., Sinninghe Damsté, J. S., 2014. Sea surface temperature variations in the western Mediterranean Sea over the last 20 kyr: A dual-organic proxy ($U^{K'}_{37}$ and LDI) approach. Paleoceanography 29, 87-98.

Rontani, J.-F., Zabeti, N., Wakeham, S.G., 2009. The fate of marine lipids: Biotic vs. abiotic degradation of particulate sterols and alkenones in the Northwestern Mediterranean Sea. Marine Chemistry 113, 9-18.

Rontani, J.-F., Volkman, J.K., Prahl, F.G., Wakeham, S.G., 2013. Biotic and abiotic degradation of alkenones and implications for $U^{K'}_{37}$ paleoproxy applications: A review. Organic Geochemistry 59, 95-113.

534   Seki, O., Schmidt, D.N., Schouten, S., Hopmans, E.C., Sinninghe Damsté, J.S., Pancost, R.D., 2012.

535   Paleoceanographic changes in the Eastern Equatorial Pacific over the last 10 Myr.

536   Paleoceanography 27, PA3224.

537   Schouten, S., Pitcher, A., Hopmans, E.C., Villanueva, L., van Bleijswijk, J., Sinninghe Damsté, J.S.,

538   2012. Intact polar and core glycerol dibiphytanyl glycerol tetraether lipids in the Arabian Sea

539   oxygen minimum zone: I. Selective preservation and degradation in the water column and

540   consequences for the TEX_{86}. Geochimica et Cosmochimica Acta 98, 228-243.

541   Shimokwara, M., Nishimura, M., Matsuda, T., Akiyama, N., Takayoshi, K., 2010. Bound forms,

542   compositional features, major sources and diagenesis of long chain, alkyl mid-chain diols in Lake

543   Baikal sediments over the past 28,000 years. Organic Geochemistry 41, 753-766.

544   Sinninghe Damsté, J.S., Rijpstra, W.I.C., Reichart, G.-J., 2002. The influence of oxic degradation on

545   the sedimentary biomarker record II. Evidence from Arabian Sea sediments. Geochimica et

546   Cosmochimica Acta 66, 2737-2754.

547   Sinninghe Damsté, J.S., Rampen, S., Rijpstra, W.I.C., Abbas, B., Muyzer, G., Schouten, S., 2003. A

548   diatomaceous origin for long-chain diols and mid-chain hydroxyl methyl alkanoates widely

549   occurring in Quaternary marine sediments: indicators for high nutrient conditions. Geochimica et

550   Cosmochimica Acta 67, 1339-1348.

551   Smith, M., De Deckker, P., Rogers, J., Brocks, J., Hope, J., Schmidt, S., Lopes dos Santos, R.,

552   Schouten, S., 2013. Comparison of $U^{K'}_{37}$, TEX^{H}_{86} and LDI temperature proxies for reconstruction

553   of south-east Australian ocean temperatures. Organic Geochemistry 64, 94-104.

554   Sun, M.-Y., Wakeham, S.G., 1994. Molecular evidence for degradation and preservation of organic

555   matter in the anoxic Black Sea Basin. Geochimica et Cosmochimica Acta 58, 3395-3406..

556   Versteegh, G.J.M., Bosch, H.J., de Leeuw, J.W., 1997. Potential palaeoenvironmental information of

557   C_{24} to C_{36} mid-chain diols, keto-ols and mid-chain hydroxy fatty acids; a critical review. Organic

558   Geochemistry 27, 1-13.

559   Versteegh, G.J.M., Jansen, J.H.F., de Leeuw, J.W., Schneider, R.R., 2000. Mid-chain diols and keto-

560   ols in SE Atlantic sediments: a new tool for tracing past sea surface water masses? Geochimica et

561   Cosmochimica Acta 64, 1879-1892.

562   Versteegh, G.J.M., Zonneveld, K.A.F., de Lange, G.J., 2010. Selective aerobic and anaerobic

563   degradation of lipids and palynomorphs in the Eastern Mediterranean since the onset of sapropel

564   S1 deposition. Marine Geology 278, 177-192.

565   Villanueva, J., Grimalt, J.O., 1997. Gas chromatographic tuning of the $U^{K'}_{37}$ paleothermometer.

566   Analytical Chemistry 69, 3329-3332.

567   Volkman, J.K., Barrett, S.M., Dunstan, G.A., Jeffrey, S.W., 1992. C_{30}–C_{32} alkyl diols and unsaturated

568   alcohols in microalgae of the class *Eustigmatophyceae*. Organic Geochemistry 18, 131-138.

569   Volkman, J.K., Barrett, S.M., Blackburn, S.I., 1999. Eustigmatophyte microalgae are potential sources

570   of C_{29} sterols, C_{22}–C_{28} n-alcohols and C_{28}–C_{32} n-alkyl diols in freshwater environments. Organic

571   Geochemistry 30, 307-318.

572   Wakeham, S.G., Peterson, M.L., Hedges, J.I., Lee, C., 2002. Lipid biomarker fluxes in the Arabian

573   Sea, with a comparison to the equatorial Pacific Ocean. Deep-Sea Research Part II 49, 2265-2301.

574   Willmott, V., Rampen, S.W., Domack, E., Canals, M., Sinninghe Damsté, J.S., Schouten, S., 2010.

575   Holocene changes in *Proboscia* diatom productivity in shelf waters of the north-western Antarctic

576   Peninsula. Antarctic Science 22, 3-10.

577

Figure Captions

Fig. 1. (a) Location of the Murray Ridge in the North Arabian Sea with the surface sediments studied (from Lengger et al, 2014). Bathymetric contour lines are at 100 m intervals. (b) Schematic illustration of the Murray Ridge with the sampling stations at different water depths. The blue area indicates the OMZ and the dashed blue line the suboxic area just below the OMZ (oxygen concentrations $>15 < 27$ µmol/L). The bottom water oxygen concentration (BWO, µmol/L) profile from Koho et al. (2013) is drawn.
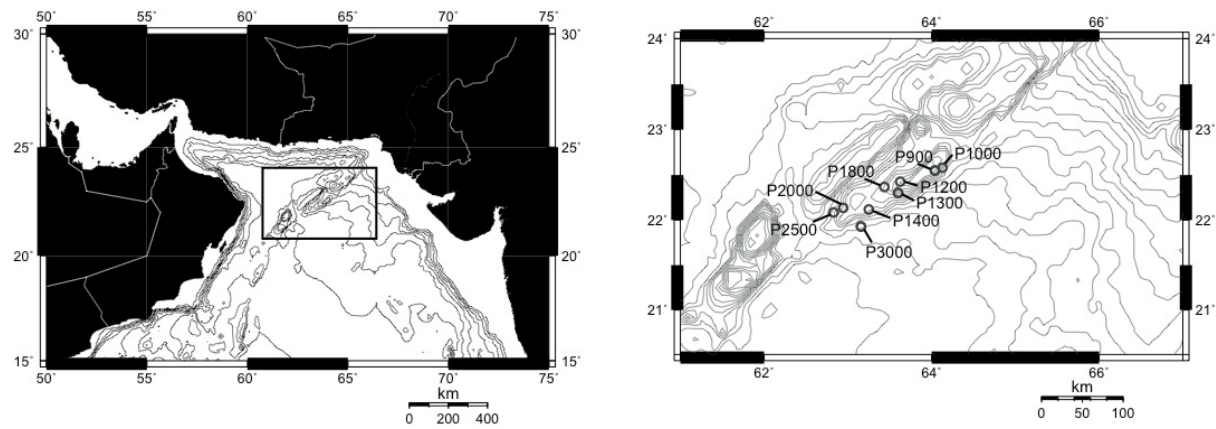
Fig. 2. Profiles of different parameters in the surface sediments (0.5 cm) from the Murray Ridge plotted with water depth. (a) organic carbon content (mg/g), (b) diol concentrations (µg/g), (c) LDI-diol concentrations (µg/g), (d) summed 1,15-, 1,14- and 1,13-diol concentrations (µg/g), (e) C_{30}-C_{34} 1,15 keto-ol concentrations (µg/g), and (f) individual C_{37} alkenone concentrations (µg/g).

Fig. 3. Indices determined in the surface sediments (0.5 cm) from the Murray Ridge. (a) $U^{K'}_{37}$ and LDI indices, (b) Upwelling indices (1,15 upw = 1,14-diols over 1,14- + 1,15-diols, cf. Rampen et al., 2008; and 1,13 upw = 1,14-diols over 1,14- + 1,13-diols, cf. Willmott et al., 2010), and (c) DOXI indices based on 1,15-diols and 1,15-keto-ols (Ferreira et al., 2001). Error bars represent duplicate analysis.

Fig. 4. Cross-plots of the residence time in the oxic zone of the sediment (t_{OZ}) expressed in years (yr) with (a) LDI, (b) C_{30} 1,15-diol concentration (µg/g), (c) C_{28}-C_{30} 1,13-diol concentrations (µg/g), (d) 1,15 upw, (e) 1,13 upw, (f) C_{28}-C_{30} 1,14-diol concentrations (µg/g), (g) $U^{K'}_{37}$, (h) $C_{37:3}$ alkenone concentration (µg/g), (i) $C_{37:2}$ alkenone concentration (µg/g). Error bars represent duplicate analysis.

Fig. 5. Bars plot of relative preservation efficiency (RPE) (i.e. relative amount in oxic sediment versus anoxic sediment, in %) of (a) diols, (b) individual C_{37} alkenones, and (c) keto-ols. Error bars represent duplicate analysis.

a)

b)

Bottom water oxygen concentration (μmol/L)

Arabian Sea

NE-SW

OMZ

Suboxic

Oxic

Murray Ridge

P900
P1000
P1200
P1300
P1500
P1800
P2000
P2500
P3000

10 km

Water depth (m)

a) $y = -0.0003x + 0.93$
$R^2 = 0.86$

b) $y = -0.0196x + 3.7$
$R^2 = 0.92$

c) C_{30} 1,13-diol
$y = -0.0007x + 0.142$
$R^2 = 0.96$

C_{28} 1,13-diol
$y = -0.0005x + 0.1098$
$R^2 = 0.95$

e) $y = -0.0002x + 0.97$
$R^2 = 0.87$

f) C_{30} 1,14-diol
$y = -0.023x + 4.35$
$R^2 = 0.95$

C_{28} 1,14-diol
$y = -0.02x + 3.82$
$R^2 = 0.94$

h) $y = -0.003x + 0.55$
$R^2 = 0.94$

i) $y = -0.06x + 12.3$
$R^2 = 0.98$